

LETTER

The quasi-lattice site-mixing model: The binary, symmetrical case

R. K. STOESELL

Department of Geology and Geophysics, University of New Orleans, New Orleans, LA 70148, U.S.A.

(Received February 13, 1989; accepted in revised form May 22, 1989)

Abstract—The quasi-chemical approximation in the quasi-chemical model was replaced with an empirical algorithm which satisfies mixing constraints not satisfied by the approximation. Unlike the quasi-chemical model, this “quasi-lattice” model will predict unmixing within the miscibility gap rather than a metastable composition with a positive free energy of mixing. For a solid solution (in which the exchange energy in each model is fixed by the critical temperature) the two different models can predict similar miscibility gaps and values of thermodynamic parameters on the boundaries, indicating a lack of sensitivity to the site-mixing algorithms for these compositions. Temperature and compositional dependencies of the exchange energy are proposed to provide modifications of the predicted miscibility gap compositions.

INTRODUCTION

COMMONLY USED solid solution site-mixing models in geochemistry include the ideal model for random site mixing (e.g., AAGAARD and HELGESON, 1983; PRICE, 1985), the regular solution model for solid solutions with insignificant deviations from random mixing (e.g., STOESELL, 1979, 1984) and the quasi-chemical model of GUGGENHEIM (1952) to handle deviations from random site mixing (e.g., GREEN, 1970; STOESELL, 1981). In addition, there is the method of BETHE (1935) which is equivalent to the quasi-chemical model and some of its elaborate and complex extensions such as the cluster variation model (BURTON and KIKUCHI, 1984).

This study utilizes the statistical mechanical formulation of the quasi-chemical model but with a different algorithm for the number of distinguishable configurations due to site mixing of “A” and “B” atoms. This empirical algorithm, unlike the quasi-chemical algorithm, does not predict negative configurational entropies of mixing as the mole fraction of AB adjacent neighbor pairs deviates from the random value. The resulting binary, symmetrical model, called the quasi-lattice model, is then compared to the quasi-chemical model with and without compositional and temperature dependencies of the exchange energy.

BINARY, SYMMETRICAL SITE-MIXING MODEL

General statistical mechanical formulation and constraints

The general formulation is given by GUGGENHEIM (1952, Chapter 4). For the binary situation of mixing one mole of A and B atoms on a lattice, the molar configurational mixing partition function \bar{Q} can be approximated by

$$\bar{Q} = \bar{g} \exp(-N_{AB}W_{AB}/kT) \quad (1)$$

where \bar{g} is the degeneracy of the most probable configuration energy of mixing one mole of A and B atoms. N_{AB} is the number of pairs of adjacent A and B atoms, and W_{AB} is the exchange energy of an AB pair of atoms on adjacent sites. This is the energy difference between an AB pair and half the energy of an AA pair plus a BB pair. T is the temperature in K, and k is the Boltzmann constant (the ratio of R the gas

constant to A_v , Avogadro's number of atoms in one mole). In this study, the number of A and B atoms, N_A plus N_B is A_v , and unless otherwise stated, $N_A \leq N_B$.

From Boltzmann's relation, \bar{S}_{conf} , the molar configurational entropy for mixing is

$$\bar{S}_{\text{conf}} = k \ln \bar{g}. \quad (2)$$

And for a condensed phase, \bar{G}_{mix} , the molar Gibbs free energy for mixing can be approximated by

$$\bar{G}_{\text{mix}} = -kT \ln \bar{Q},$$

or

$$\bar{G}_{\text{mix}} = -T\bar{S}_{\text{conf}} + zX_{AB}\bar{W}_{AB}/2, \quad (3)$$

where z is the site coordination number, X_{AB} is the mole fraction of AB pairs, i.e., $N_{AB}/(N_{AA} + N_{BB} + N_{AB})$ for $(zA_v/2)$ pairs, and \bar{W}_{AB} is the molar exchange energy. The nonideal mixing terms for both entropy and enthalpy are included in the last term in Eqn. (3). In this study, several possibilities for \bar{W}_{AB} will be used. \bar{W}_{AB} is assumed constant in Eqn. (9a), a function of composition in Eqn. (9b), and a function of both composition and temperature in Eqn. (9c). X_A and X_B , used below, refer to mole fractions of A and B, respectively, in the solid composition.

The correct value of X_{AB} is that which minimizes Eqn. (3) at constant T and X_A . It is determined by solving for X_{AB} in

$$\frac{\partial \bar{G}_{\text{mix}}}{\partial X_{AB}} = 0. \quad (4)$$

As given later in Eqn. (12), there is an explicit equation for X_{AB} , determined from Eqn. (4) in the quasi-chemical model. The value in the quasi-lattice model was determined numerically using Newton's method.

Because of symmetry, the critical point composition in the symmetrical, binary system will be at $X_A = 0.5$. The critical temperature, T_c occurs when

$$\frac{\partial \bar{G}_{\text{mix}}}{\partial X_A} = \frac{\partial^2 \bar{G}_{\text{mix}}}{\partial X_A^2} = 0 \quad (5)$$

in which taking the first partial derivative is simplified by virtue of the partial derivative of X_{AB} with respect to X_A being zero. There are six cases considered in this study, three for

the quasi-chemical model and three for the quasi-lattice model (using the three different definitions of \bar{W}_{AB} in Eqns. (9a)–(9c) with each model). With the exception of the quasi-chemical model, utilizing Eqn. (9a), T_c was matched with \bar{W}_{AB} from graphical plots. In the one exception, GUGGENHEIM (1952, Chapter 4) provides an explicit relation, Eqn. (13), between the two quantities.

Additional thermodynamic parameters in the solid solution model, to be compared between the quasi-chemical and quasi-lattice models, are the activity coefficient, y_A , the molar entropy of mixing, \bar{S}_{mix} , and the molar heat capacity of mixing, $\bar{C}_{p\text{mix}}$. These quantities are computed as follows:

$$\ln y_A = \left(\bar{G}_{\text{mix}} + X_B \frac{\partial \bar{G}_{\text{mix}}}{\partial X_A} \right) / RT - \ln X_A, \quad (6)$$

$$\bar{S}_{\text{mix}} = \frac{-\partial \bar{G}_{\text{mix}}}{\partial T}, \quad (7)$$

and

$$\bar{C}_{p\text{mix}} = T \frac{\partial \bar{S}_{\text{mix}}}{\partial T}. \quad (8)$$

In this paper the $\frac{\partial \bar{G}_{\text{mix}}}{\partial X_A}$ in Eqn. (6) was determined using the analytical derivative of Eqn. (3); however, finite difference derivatives were used for the $\frac{\partial \bar{G}_{\text{mix}}}{\partial T}$ and the $\frac{\partial \bar{S}_{\text{mix}}}{\partial T}$ terms, respectively, in Eqns. (7) and (8).

Important mass balance constraints in the solid solution are:

$$\begin{aligned} N_A + N_B &= A_v, & N_{AA} + N_{BB} + N_{AB} &= zA_v/2; \\ X_A + X_B &= 1, & X_{AB} + X_{AA} + X_{BB} &= 1; \\ X_A &= X_{AA} + X_{AB}/2, & X_B &= X_{BB} + X_{AB}/2; \end{aligned}$$

and

$$0 \leq X_{AB} \leq 2X_A \quad \text{where} \quad N_A \leq N_B.$$

Mixing constraints in the solid solution include the following:

$$\begin{aligned} 0 &\leq X_{AB} < 2X_A X_B & \text{for } \bar{W}_{AB} > 0; \\ 2X_A X_B &< X_{AB} \leq 2X_A & \text{for } \bar{W}_{AB} < 0; \\ X_{AB} &= 2X_A X_B & \text{and } \bar{S}_{\text{conf}} = R(X_A \ln X_A + X_B \ln X_B), \\ & & \text{for random mixing when } \bar{W}_{AB} = 0; \\ X_{AB} &\Rightarrow 0 & \text{and } \bar{S}_{\text{conf}} \Rightarrow 0, \\ & & \text{for total unmixing as } \bar{W}_{AB} \Rightarrow +\infty; \\ X_{AB} &\Rightarrow 2X_A & \text{and } \bar{S}_{\text{conf}} \Rightarrow 0, \\ & & \text{for total order as } \bar{W}_{AB} \Rightarrow -\infty \end{aligned}$$

in which $X_A \leq X_B$;

$$\frac{\partial \bar{S}_{\text{conf}}}{\partial X_A} = 0,$$

for symmetry at $X_A = X_B$;

and with increasing departure from random mixing, \bar{S}_{conf} should decrease more rapidly from its random value, when z is larger; conversely, \bar{S}_{conf} should increase more rapidly from zero (at $X_{AB} = 0$ and $2X_A$) with smaller values of z .

The algorithm \bar{g} in Eqn. (1) describes the number of distinguishable configurations and is a direct function of X_{AB} and X_A . It is an indirect function of \bar{W}_{AB} since X_{AB} is found by minimizing \bar{G}_{mix} in Eqn. (3) with respect to X_{AB} at constant composition and temperature. Both the quasi-chemical and the quasi-lattice model (developed in this paper) for the binary symmetrical case will utilize Eqns. (1)–(3). The differences are in the assumed form of the algorithm \bar{g} and that the quasi-chemical model does not generally follow the mixing constraints for *total order* and *total unmixing*. It is important to emphasize that the correct algorithm for \bar{g} (in three dimensions) is known only for random mixing. Both the quasi-chemical and quasi-lattice algorithms are empirical algorithms that reduce to the random case when \bar{W}_{AB} is zero.

In this paper, \bar{W}_{AB} is defined in terms of \bar{W}_{AB}^* , the value at the critical temperature of mixing with or without a compositional and temperature dependence. The critical temperature T_c is the temperature above which stable mixing occurs at all compositions. Three situations will be considered: a constant value defined by Eqn. (9a), a compositional dependence defined by Eqn. (9b), and a compositional and temperature dependence defined by Eqn. (9c).

$$\bar{W}_{AB} = \bar{W}_{AB}^*, \quad (9a)$$

$$\bar{W}_{AB} = \bar{W}_{AB}^*(4X_A X_B), \quad (9b)$$

and

$$\bar{W}_{AB} = \bar{W}_{AB}^*(4X_A X_B) T_c / T. \quad (9c)$$

The compositional dependence is a multiplication factor $4X_A X_B$ which increases from zero to unity as X_A varies from 0 to 0.5, being symmetrical about $X_A = 0.5$. The temperature dependence is an additional multiplication factor T_c/T which decreases to unity and below as the temperature rises and passes the critical temperature. These factors are empirical, yet they do have a certain common sense to them. If site mixing causes lattice distortion (*i.e.*, for positive \bar{W}_{AB}) we would expect the distortion to be at a maximum when X_A is 0.5 and to approach zero as X_A or X_B approaches zero. Similarly, because of lattice expansion with increasing temperature, we would expect the relative distortion due to mixing to be less significant with increasing temperature.

Symmetrical quasi-chemical model

The symmetrical, binary quasi-chemical model was developed by GUGGENHEIM (1952, Chapter 4). In this discussion, only the assumptions will be given together with Guggenheim's results. The notation of W and X used by Guggenheim are equal, respectively, to (zW_{AB}) and N_{AB}/z in this study. His model is based on the assumption that the number of configurations is proportional to the number of configurations resulting from mixing pairs of sites without regard for the fact that each site is included in more than one pair of sites.

For a particular value of X_{AB} , \bar{g} is set equal to the number of configurations resulting from random mixing times a normalization factor. The normalization factor sets \bar{g} to that of random mixing of atoms when \bar{W}_{AB} is equal to zero but generally not to unity when $\bar{W}_{AB} \Rightarrow +\infty$ or $-\infty$. The result is that \bar{G}_{mix} is generally not zero when X_{AB} is 0 or $2X_A$ for $X_A \leq X_B$. For these cases, the quasi-chemical model does not predict $X_{AB} \Rightarrow$ zero with increasing values of positive \bar{W}_{AB} relative to T .

From GUGGENHEIM (1952, Chapter 4), \bar{g} in the quasi-chemical model becomes

$$\bar{g} = \left[\frac{(N_A + N_B)!}{N_A! N_B!} \right] \left[\frac{N_{AA}^*! N_{BB}^*! ((N_{AB}^*/2)!)^2}{N_{AA}! N_{BB}! ((N_{AB}/2)!)^2} \right]. \quad (10)$$

Note that the first bracketed set of terms is just the number of configurations due to random mixing of A and B atoms. The * terms in the numerator of the second bracketed are the random mixing values of the terms in the denominator. They are computed assuming random mixing of pairs, neglecting the fact that each site is shared with z pairs. The denominator terms are solved for by using the constraint of Eqn. (4) and the mass balance relations.

From Eqns. (2) and (10), \bar{S}_{conf} becomes for the binary, symmetrical case:

$$\begin{aligned} \bar{S}_{\text{conf}} = & -R(X_A \ln X_A + X_B \ln X_B) + \frac{z}{2} R(X_A^2 \ln X_A^2 \\ & + 2X_A X_B \ln(X_A X_B) + X_B^2 \ln X_B^2) - X_{AA} \ln X_{AA} \\ & - X_{AB} \ln \frac{X_{AB}}{2} - X_{BB} \ln X_{BB}. \end{aligned} \quad (11)$$

\bar{G}_{mix} is found by substituting Eqn. (11) into Eqn. (3). X_{AB} is determined using Eqn. (4), resulting in

$$X_{AB} = \frac{1 - (1 - 4X_A X_B (1 - \exp(2\bar{W}_{AB}/RT))^{1/2}}{1 - \exp(2\bar{W}_{AB}/RT)}. \quad (12)$$

One of the most useful aspects of the quasi-chemical model is that Eqns. (2), (11), and (12), together with the previously given mass balance constraints, provide an explicit expression for \bar{G}_{mix} in Eqn. (3). There is no need to resort to a numerical solution for \bar{G}_{mix} .

Equation (13) is from GUGGENHEIM (1952, Chapter 4) and provides a relation between \bar{W}_{AB} and T_c in $^\circ\text{K}$ when \bar{W}_{AB} is a constant, defined by Eqn. (9a):

$$\bar{W}_{AB} = RT_c \ln(z/(z-2)). \quad (13)$$

All other thermodynamic parameters in the quasi-chemical model were computed using Eqns. (6)–(8) as discussed in the previous section.

Symmetrical quasi-lattice model

The algorithm \bar{g} , presented below, is an empirical expression that satisfies the previously mentioned mixing relations, including those not satisfied by the quasi-chemical model. The basis of the algorithm is the assumption that the number of distinguishable configurations can be computed using a random site-mixing model in which the lattice size decreases

as X_{AB} deviates from its random value of $2X_A X_B$. The idea is that a certain number of sites on the lattice are reserved for A and B occupancies in order to have a particular value of X_{AB} . These sites are removed from the random site-mixing algorithm, and the number removed will increase as X_{AB} approaches zero or $2X_A$.

Accordingly, \bar{g} could be represented by Eqn. (14).

$$\bar{g} = \frac{((N_A + N_B)h)!}{(N_A h)!(N_B h)!} \quad (14)$$

where $N_A \leq N_B$ and h is a function of X_A and X_{AB} . Substitution of Eqn. (14) into Eqn. (2) yields

$$\bar{S}_{\text{conf}} = -Rh(X_A \ln X_A + X_B \ln X_B). \quad (15)$$

Mixing constraints require h satisfy the following conditions:

$$h = 1 \quad \text{when} \quad X_{AB} = 2X_A X_B,$$

$$h = 0 \quad \text{when} \quad X_{AB} = 0 \quad \text{and} \quad X_{AB} = 2X_A,$$

$$\frac{\partial h}{\partial X_{AB}} = 0 \quad \text{when} \quad X_{AB} = 2X_A X_B,$$

$$\frac{\partial h}{\partial X_{AB}} = +\infty \quad \text{when} \quad X_{AB} = 0, \quad \text{and}$$

$$\frac{\partial h}{\partial X_{AB}} = -\infty \quad \text{when} \quad X_{AB} = 2X_A.$$

In this study, h has been set equal to the sum of two equations: h_1 , a quadratic equation containing a “1n” term to satisfy the above “infinity conditions” and h_2 , a cubic equation added to provide a functional dependency of z . The minimum z value of 2 sets h_2 equal to zero in the summation.

$$h = h_1 + h_2 \quad (16)$$

Both h_1 and h_2 satisfy the constraints for h except that at $X_{AB} = 0$ and $2X_A$, h_2 has a partial derivative of zero, and at $X_{AB} = 2X_A X_B$, h_1 and $h_2 = 2/z$ and $(z-2)/z$, respectively. Coefficients in Eqns. (17)–(20) below were determined with those constraints.

For the region $0 \leq X_{AB} \leq 2X_A X_B$ (i.e., $\bar{W}_{AB} \geq 0$):

$$\begin{aligned} h_1 = & X_{AB} \ln \left[\frac{2X_A X_B}{X_{AB}} \right] + \frac{(2 - zX_A X_B)}{zX_A X_B} X_{AB} \\ & + \frac{(zX_A X_B - 1)}{2z(X_A X_B)^2} X_{AB}^2, \end{aligned} \quad (17)$$

and

$$h_2 = \frac{3(z-2)}{z(2X_A X_B)^2} X_{AB}^2 - \frac{2(z-2)}{z(2X_A X_B)^3} X_{AB}^3. \quad (18)$$

For the region $2X_A X_B \leq X_{AB} \leq 2X_A$ (i.e., $\bar{W}_{AB} \leq 0$):

$$\begin{aligned} h_1 = & (2X_A - X_{AB}) \ln \left[\frac{2X_A^2}{2X_A - X_{AB}} \right] + \frac{(2 - zX_A^2)}{zX_A^2} \\ & \times (2X_A - X_{AB}) + \frac{(zX_A^2 - 1)}{2zX_A^4} (2X_A - X_{AB})^2 \end{aligned} \quad (19)$$

and

$$h_2 = \frac{3(z-2)}{4zX_A^4} (2X_A - X_{AB})^2 - \frac{(z-2)}{4zX_A^6} (2X_A - X_{AB})^3. \quad (20)$$

\bar{G}_{mix} is defined using Eqns. (15) and (16) and, depending upon \bar{W}_{AB} , either Eqns. (17) and (18) or Eqns. (19) and (20) in Eqn. (3). The correct value of X_{AB} to use in Eqn. (3) was found numerically with Newton's method with Eqn. (4). All other thermodynamic parameters were computed using Eqns. (4)–(8) as previously discussed.

RESULTS AND DISCUSSION

\bar{S}_{conf} values are plotted for the quasi-chemical model and the quasi-lattice model on Figs. 1 and 2, respectively, as a function of X_{AB} . On Figs. 1a and 2a, the curves represent different values of z at a solid solution composition of $0.5X_A$. On Figs. 2a and 2b, the curves represent different compositions at a z of 6. Values of \bar{S}_{conf} predicted by the quasi-chem-

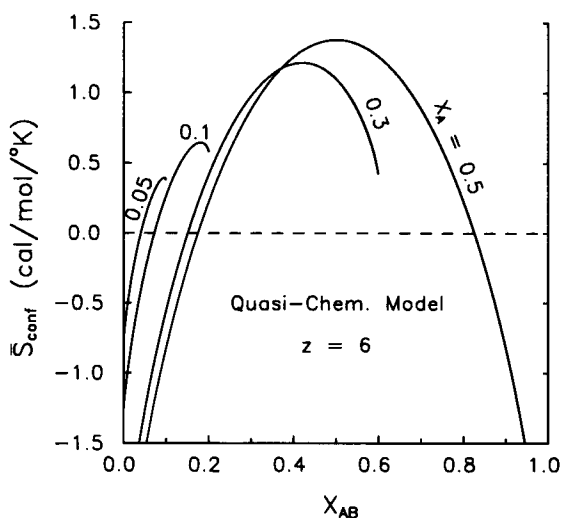
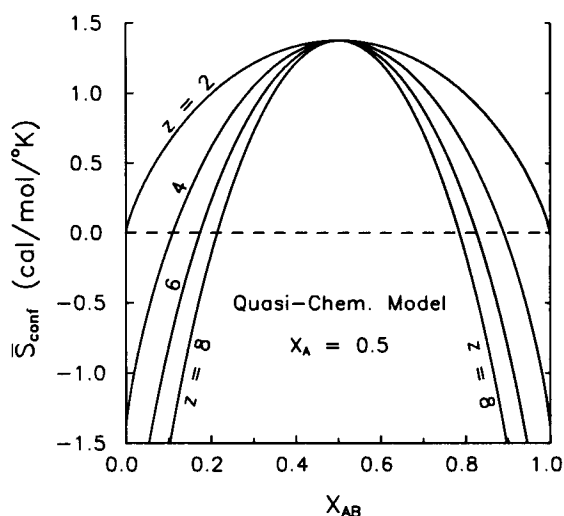


FIG. 1. \bar{S}_{conf} versus X_{AB} for the quasi-chemical model: (a) for different values of z at X_A equal to 0.5; (b) for different compositions at z equal to 6.

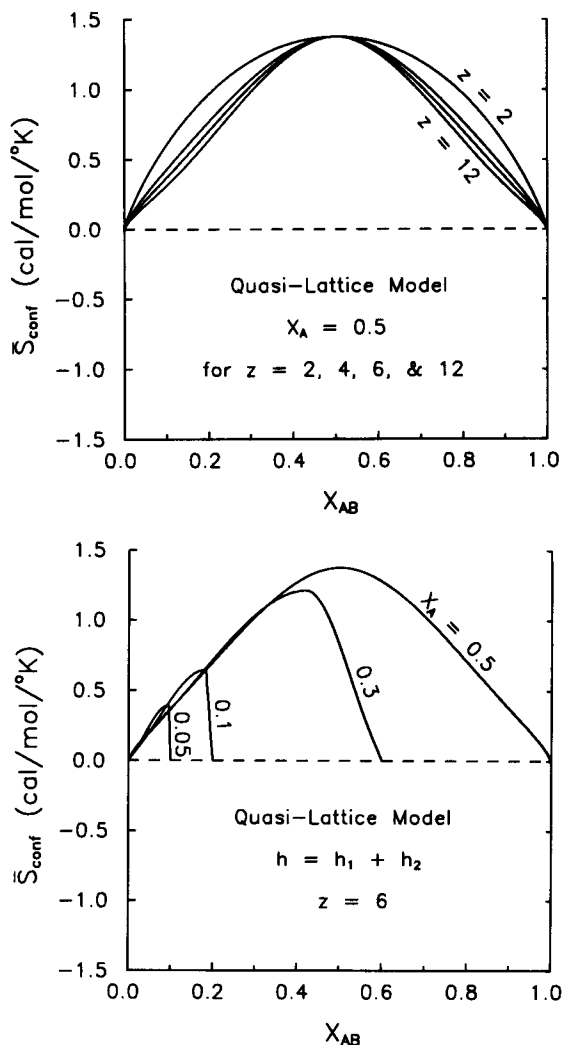


FIG. 2. \bar{S}_{conf} versus X_{AB} for quasi-lattice model: (a) for different values of z at X_A equal to 0.5; (b) for different compositions at z equal to 6.

ical model can be negative and generally do not approach zero as X_{AB} approaches zero or $2X_A$. Values of \bar{S}_{conf} predicted by the quasi-lattice model are always positive and do approach zero as X_{AB} approaches zero or $2X_A$. Although the quasi-lattice model obeys all the mixing constraints (unlike the quasi-chemical model), the minor functional dependence of \bar{S}_{conf} on z indicates the algorithm could be further improved.

The potential for negative \bar{S}_{conf} causes the quasi-chemical model to predict a larger X_{AB} for a given composition than does the quasi-lattice model. This prevents the quasi-chemical model from predicting X_{AB} approaching zero with increasing \bar{W}_{AB} . The result, as shown on Fig. 3, is that the quasi-chemical model predicts positive \bar{G}_{mix} with nonzero X_{AB} when the quasi-lattice model predicts \bar{G}_{mix} approaching zero with X_{AB} approaching zero.

On Fig. 3, \bar{G}_{mix} is plotted versus composition at 500°C for the two models using the three definitions for \bar{W}_{AB} , given in Eqns. (9a), (9b), and (9c) and a z value of 6. The value of \bar{W}_{AB}^* in each situation has been fixed by assuming a common critical temperature of 1150°C . The z and T_c correspond to that of the disordered, binary, asymmetrical rhombohedral

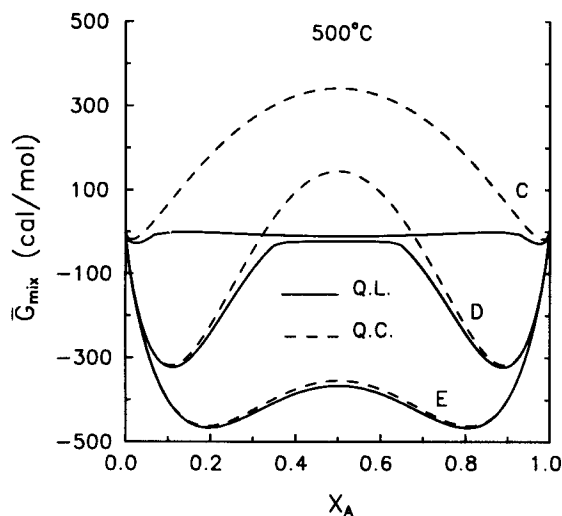


FIG. 3. \bar{G}_{mix} versus X_A at 500°C for the quasi-lattice model (solid curves) and the quasi-chemical model (dashed curves) with $z = 6$, $T_c = 1150^\circ\text{C}$, and \bar{W}_{AB} defined by: Eqn. (9a), curves C; Eqn. (9b), curves E; and Eqn. (9c), curves D. \bar{W}_{AB}^* values in (cal/mol) are: 1,167.946, solid curve C; 1,146.689, dashed curve C; 517.170, solid curves D and E; and 517.195, dashed curves D and E. The values are explained in the text.

carbonate system, $\text{Ca}_x\text{Mg}_{(1-x)}\text{CO}_3$ (REEDER and NAKAJIMA, 1982). This system is one which the author will attempt to model in a later publication with an asymmetrical, binary quasi-lattice model. The parameters are used here because the low temperature arm for $X_A < 0.5$ of the "D" curves, defining the immiscibility gap on Fig. 4, is close to that expected for the calcite arm with magnesite (component A) dissolved in calcite (component B), *e.g.*, see GOLDSMITH (1983, Figs. 9 and 10).

The procedure followed in determining \bar{W}_{AB}^* , with one exception, was to find (graphically) the largest \bar{W}_{AB}^* at T_c that would produce a concave curve of \bar{G}_{mix} versus X_A at X_A equal to 0.5. The one exception was the quasi-chemical model with \bar{W}_{AB}^* defined by Eqn. (9a) for which Eqn. (13) can be used to directly calculate \bar{W}_{AB}^* . Because Eqns. (9b) and (9c) are equivalent at T_c , those \bar{W}_{AB}^* values are the same for a particular model. \bar{W}_{AB}^* values are reported below in cal/mol where a calorie is equivalent to 4.184 joules. For the quasi-chemical model, the \bar{W}_{AB}^* values, used on Figs. 3–7, are 1,146.689 cal/mol for \bar{W}_{AB}^* defined by Eqn. (9a) and 517.195 cal/mol for \bar{W}_{AB}^* defined by Eqns. (9b) and (9c). The corresponding values for the quasi-lattice model are 1,167.946 and 517.170 cal/mol, respectively.

On Fig. 3, \bar{G}_{mix} decreases at constant composition, going from \bar{W}_{AB} being a constant (curves C), a function of both temperature and composition (curves D), and a function of composition (curves E). The trend is due to a decrease in the computed \bar{W}_{AB} values in Eqns. (9a), (9c), and (9b), respectively. In addition, for each family of two curves, \bar{G}_{mix} is more positive in the quasi-chemical model (dashed curve) than in the quasi-lattice model (solid curve). However, these differences are insignificant outside of the miscibility gap.

In Fig. 4, the boundaries of the miscibility gap are plotted for the quasi-chemical model (dashed curves) and the quasi-lattice model (solid curves) for each of the three cases defining

\bar{W}_{AB} : curves C (Eqn. 9a), curves D (Eqn. 9c), and curves E (Eqn. 9b). The boundaries of the miscibility gaps were determined graphically using \bar{G}_{mix} plots versus X_A as on Fig. 3. The differences between miscibility gaps between the two models are nearly insignificant within each family of curves, *i.e.*, between the dashed and solid curves for C, D, and E. The differences in \bar{S}_{conf} between the two models, shown on Figs. 1 and 2, have an insignificant effect on the location of the miscibility gap boundaries. There is a much greater effect on the position of these boundaries due to the method used in computing \bar{W}_{AB} : holding it constant (curves C), having a compositional dependence (curves E), or having both a temperature and compositional dependence (curves D). As expected, the larger the \bar{W}_{AB} value, the wider is the miscibility gap.

Several additional thermodynamic properties: the $\ln y_A$, the \bar{S}_{mix} and the \bar{C}_p are plotted, respectively, on Figs. 5, 6, and 7 as a function of temperature along the miscibility gap shown in Fig. 4. These were computed, as previously discussed, using Eqns. (6), (7), and (8). Again, the major point is that the differences in predicted thermodynamic properties between the two models are insignificant along the boundaries of the miscibility gap with the possible exception of \bar{C}_p on Fig. 7. As expected, from Fig. 4, the predicted thermodynamic properties are highly dependent upon the method used to compute \bar{W}_{AB} , as indicated by differences between the C, D, and E curves on each figure.

An asymmetrical binary model is under development for the quasi-lattice model and will be compared with the quasi-chemical model in a later publication. Guggenheim's asymmetrical form of the quasi-chemical model is based on mixing monomers, dimers (and other polymer species) on the sites (GUGGENHEIM, 1952, Chapter 11). GREEN (1970) successfully used Guggenheim's formulation to model the NaCl-KCl system. The form of the asymmetrical quasi-lattice model under development has asymmetrical expressions for both \bar{g} and \bar{W}_{AB} in which the asymmetry is a function of X_A^* , the critical composition at T_c . The asymmetrical, binary quasi-lattice model will reduce directly to the symmetrical model of this study when $X_A^* = 0.5$.

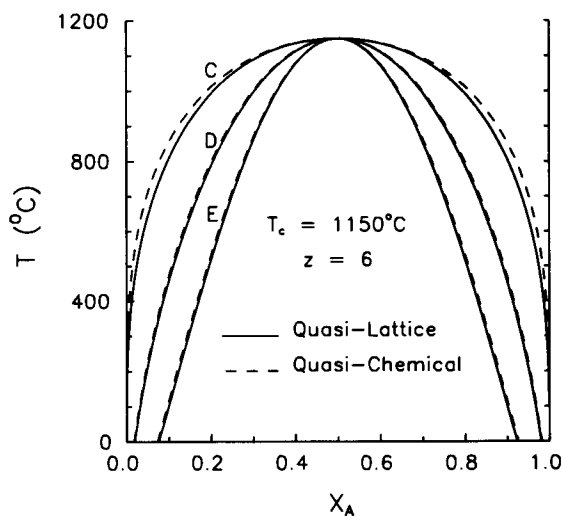


FIG. 4. Immiscibility boundary compositions for the binary system with the curve parameters listed in caption for Fig. 3.

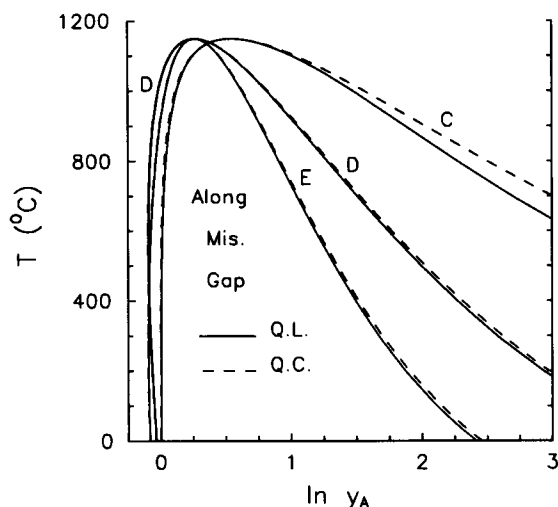


FIG. 5. Temperature versus $\ln y_A$ along the immiscibility boundary curves shown in Fig. 4 using the parameters listed in Fig. 3. The left legs of the curves on Fig. 4 correspond to the right legs of the curves on Fig. 5 and vice versa.

SUMMARY

An empirical, alternative site-mixing algorithm to the quasi-chemical algorithm is proposed for a binary, symmetrical model. The resulting model, the quasi-lattice model, satisfies mixing constraints when X_{AB} is far from its random value of $2X_A X_B$. These mixing constraints are not satisfied by the quasi-chemical model. The exchange energies in both models were modified by proposed compositional and temperature dependencies which should prove useful in modeling real systems with the asymmetric forms of the models.

A comparison of predicted values of \bar{G}_{mix} , \bar{S}_{mix} , $\bar{C}p_{\text{mix}}$, and the composition boundary of the miscibility gap was made for a binary system with a z value of 6, a T_c of 1150°C , and with and without compositional and temperature dependencies of \bar{W}_{AB} . While, there are major differences between the two models within the miscibility gap, the differences were insignificant along the boundaries of the miscibility gap, indicating an insensitivity in the binary, symmetrical

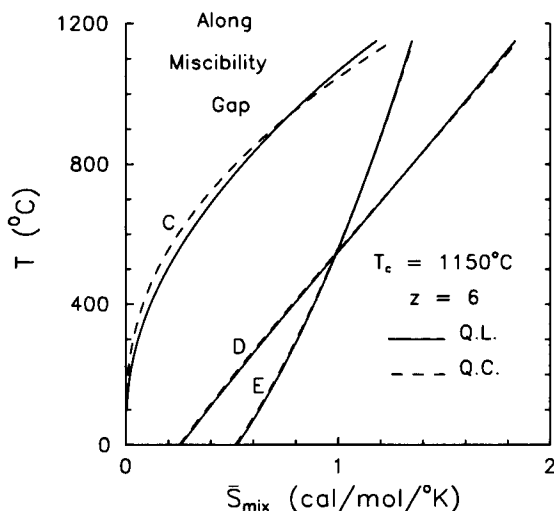


FIG. 6. Temperature versus \bar{S}_{mix} along the immiscibility boundary curves shown in Fig. 4 using the parameters listed in Fig. 3.

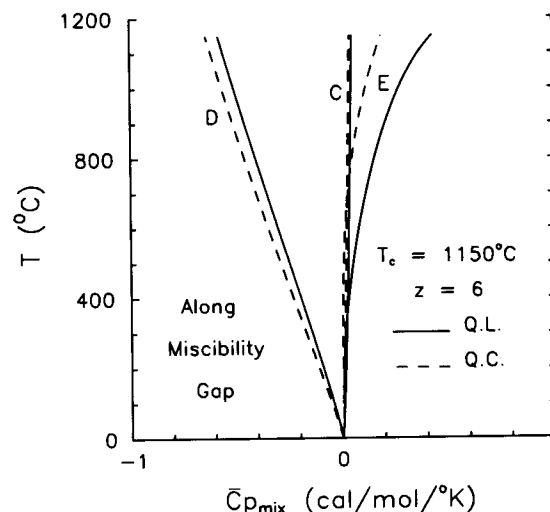


FIG. 7. Temperature versus $\bar{C}p_{\text{mix}}$ along the immiscibility boundary curves shown in Fig. 4 using the parameters listed in Fig. 3.

case to the site-mixing algorithms for these compositions. Predictions from both models were very sensitive to the proposed temperature and composition dependencies of \bar{W}_{AB} . An asymmetrical form of the binary, symmetrical quasi-lattice model is in preparation and will be used in a later publication to model various binary carbonate systems.

Acknowledgements—The study was made possible by sabbatical salary support and the use of a Zenith 386 PC provided by the Department of Geology and Geophysics at the University of New Orleans. The author would like to thank Benjamin Burton and Jonathan Price, the journal reviewers, for their constructive comments.

Editorial handling: P. C. Hess

REFERENCES

- AAGAARD P. and HELGESON H. C. (1983) Activity/composition relations among silicates and aqueous solutions: II. Chemical and thermodynamic consequences of ideal mixing of atoms on homological sites in montmorillonites, illites, and mixed-layer clays. *Clays Clay Minerals* **31**, 207–217.
- BETHE H. A. (1935) Statistical theory of superlattices. *Proc. Roy. Soc. London* **A150**, 552–575.
- BURTON B. and KIKUCHI R. (1984) Thermodynamic analysis of the system $\text{CaCO}_3\text{-MgCO}_3$ in the tetrahedron approximation of the cluster variation method. *Amer. Mineral.* **69**, 165–175.
- GOLDSMITH J. R. (1983) Phase relations of rhombohedral carbonates. In *Carbonates: Mineralogy and Chemistry* (ed. R. J. REEDER); *Reviews in Mineralogy*, vol. 11, pp. 49–76. Mineral. Soc. Amer., Washington D.C.
- GREEN E. J. (1970) Predictive thermodynamic models for mineral systems. I. Quasi-chemical analysis of the halite-sylvite subsolidus. *Amer. Mineral.* **55**, 1692–1713.
- GUGGENHEIM E. A. (1952) *Mixtures*. Clarendon Press, Oxford, 270p.
- PRICE J. G. (1985) Ideal site mixing in solid solutions, with an application to two-feldspar geothermometry. *Amer. Mineral.* **70**, 696–701.
- REEDER R. J. and NAKAJIMA Y. (1982) The nature of ordering and ordering defects in dolomite. *Physics and Chemistry of Minerals* **8**, 29–35.
- STOESSELL R. K. (1979) A regular solution site-mixing model for illites. *Geochim. Cosmochim. Acta* **43**, 1151–1159.
- STOESSELL R. K. (1981) Refinements in a site-mixing model for illites: Local electrostatic balance and the quasi-chemical approximation. *Geochim. Cosmochim. Acta* **45**, 1733–1741.
- STOESSELL R. K. (1984) A regular solution site-mixing model for chlorites. *Clays Clay Minerals* **32**, 205–212.